Published in final edited form as:
Neuroscience. 2010 September 29; 170(1): 78–91. doi:10.1016/j.neuroscience.2010.06.068.

DISTINCT TYPES OF NON-CHOLINERGIC PEDUNCULOPONTINE NEURONS ARE DIFFERENTIALLY MODULATED DURING GLOBAL BRAIN STATES

H. ROŠ[1], **P. J. MAGILL**, **J. MOSS**[2], **J. P. BOLAM**, and **J. MENA-SEGOVIA**[*]
Medical Research Council Anatomical Neuropharmacology Unit, Department of Pharmacology, University of Oxford, Mansfield Road, Oxford OX1 3TH, UK

Abstract

The pedunculopontine nucleus (PPN) is critically involved in brain-state transitions that promote neocortical activation. In addition, the PPN is involved in the control of several behavioral processes including locomotion, motivation and reward, but the neuronal substrates that underlie such an array of functions remain elusive. Here we analyzed the physiological properties of non-cholinergic PPN neurons *in vivo* across distinct brain states, and correlated these with their morphological properties after juxtacellular labeling. We show that non-cholinergic neurons in the PPN whose firing is not strongly correlated to neocortical activity are highly heterogeneous and are composed of at least three different subtypes: (1) “quiescent” neurons, which are nearly silent during slow-wave activity (SWA) but respond robustly to neocortical activation; (2) “tonic firing” neurons, which have a stationary firing rate that is independent of neocortical activity across different brain states; and (3) “irregular firing” neurons, which exhibit a variable level of correlation with neocortical activity. The majority of non-cholinergic neurons have an ascending axonal trajectory, with the exception of some irregular firing neurons that have descending axons. Furthermore, we observed asymmetric synaptic contacts within the PPN arising from the axon collaterals of labeled neurons, suggesting that excitatory, non-cholinergic neurons can shape the activity of neighboring cells. Our results provide the first evidence of distinct firing properties associated with non-cholinergic neuronal subtypes in the PPN, suggesting a functional heterogeneity, and support the notion of a local network assembled by projection neurons, the properties of which are likely to determine the output of the PPN in diverse behavioral contexts.

Keywords

pedunculopontine; cortical slow oscillations; cholinergic; basal ganglia; neocortex; local network

Global brain-state transitions are predominantly driven by widespread-projecting neurons of a subset of structures located in the brainstem. One such brainstem structure is the

[*]Corresponding author. Tel: +44-1865-271870; fax: +44-1865-271647. juan.mena-segovia@pharm.ox.ac.uk (J. Mena-Segovia).
[1]Present address: Department of Neuroscience, Physiology and Pharmacology, University College London, 323 Rockefeller Building, 21 University Street, London, WC1E 6DE, UK.
[2]Present address: Center for Molecular and Behavioral Neuroscience, Rutgers University, 197 University Avenue, Newark, NJ 07102, USA.

Europe PMC Funders Author Manuscripts

pedunculopontine nucleus (PPN), whose long axons extend to wide areas of the forebrain producing modulation and/or activation of distal neuronal systems (e.g. thalamus-cortex, basal ganglia, basal forebrain). Until recently, the PPN and related areas, conceptually grouped as the reticular activating system (RAS), were considered to be relay structures with homogeneous patterns of discharge and whose primary function was to produce activation of the forebrain and ultimately the neocortex (Steriade and McCarley, 2005). The notion of the PPN as a part of the RAS is based on the functional properties of presumed cholinergic neurons whose activity is enhanced during brain cortical activation (i.e. during wakefulness and rapid eye movement [REM] sleep) and reduced during slow-wave activity (SWA; i.e. during sleep and anesthesia) (for reviews see Jones, 2005; Saper et al., 2005; McCarley, 2007). A close link between cortical brain states and PPN activity has been well documented by experiments eliciting cortical activation through electrical stimulation of the PPN (Steriade et al., 1991; Curto et al., 2009), and by recordings *in vivo* showing increased firing rate of identified cholinergic neurons during spontaneous or sensory-induced brain state transitions (Mena-Segovia et al., 2008). The conceptual notion of the RAS is also supported by the fact that cholinergic neurons represent a relatively homogeneous population, both in terms of their morphological and physiological properties. The great majority of identified cholinergic PPN neurons (80%) discharge during the active component of neocortical slow oscillations (Up state) and all of them increase their firing rate during transitions from SWA to activated brain states (Mena-Segovia et al., 2008).

Increasing evidence supports the involvement of the PPN in other diverse behavioral processes, ranging from locomotion and gait (Garcia-Rill et al., 1987; Nandi et al., 2002; Takakusaki et al., 2003), to addiction (Corrigall et al., 2002; Maskos, 2008) and reward (Ainge et al., 2006; Heinmiller et al., 2009; Okada et al., 2009). Regions associated with such behaviors respond to both a cholinergic component originating in the PPN, and a PPN-mediated non-cholinergic component, presumably arising from non-cholinergic PPN neurons (Good and Lupica, 2009). Recent estimates show that non-cholinergic neurons comprise more than 80% of all PPN neurons in the rat, and include populations of GABAergic and glutamatergic neurons, both of which account for twice the number of cholinergic neurons (Mena-Segovia et al., 2009; Wang and Morales, 2009). Further evidence supporting a functional divergence between identified neuronal subtypes is that a subpopulation of non-cholinergic PPN neurons, whose firing is temporally correlated with neocortical slow oscillations, maintains a phase coupling which is more than 90° shifted from that of the cholinergic neurons (Mena-Segovia et al., 2008). This suggests a distinct afferent modulation and thus a different contribution to their target structures. Therefore, one possibility that might explain the functional heterogeneity of the PPN is the emergent properties and diversity of its non-cholinergic neurons. To investigate this possibility, we recorded and labeled PPN neurons during different brain states *in vivo* using the juxtacellular method, and analyzed their electrophysiological and morphological characteristics during spontaneous and evoked transitions of global brain state.

EXPERIMENTAL PROCEDURES

Electrophysiological recordings

Experiments were carried out on 53 adult male Sprague–Dawley rats (250–310 g; Charles River, Margate, UK) in accordance with the Animals (Scientific Procedures) Act, 1986 (UK). Anesthesia was induced with 4% v/v isofluorane (Isoflo, Schering-Plough, Welwyn Garden City, UK) in O_2, and maintained with urethane (1.3 g/kg i.p.; ethyl carbamate; Sigma, Poole, UK), and supplemental doses of ketamine (30 mg/kg i.p.; Ketaset, Willows Francis, Crawley, UK) and xylazine (3 mg/kg i.p.; Rompun, Bayer, Germany), as described previously (Magill et al., 2004). Electrocardiographic activity, respiration rate, the electrocorticogram (ECoG; see below) and reflexes were monitored to ensure the animals' well-being. Body temperature was maintained at 37 °C by a feedback temperature controller.

The ECoG was recorded via a 1 mm diameter steel screw juxtaposed to the dura mater above the frontal cortex (3.0 mm anterior and 2.5 mm lateral of bregma; Paxinos and Watson, 1986), which corresponds to the somatic sensorimotor cortex (Donoghue and Wise, 1982). The raw ECoG signal was band-pass filtered (0.3–1500 Hz, −3 dB limits) and amplified (2000×; DPA-2FS filter/amplifier; Scientifica, Harpenden, UK) before acquisition. Extracellular recordings of action potentials of individual PPN neurons were made using 15–25 MΩ glass electrodes (tip diameter ~1.5 μm), filled with saline solution (0.5 M NaCl) and neurobiotin (1.5% w/v, Vector Laboratories Ltd., Peterborough, UK). Glass electrode signals were amplified (10×) through the active bridge circuitry of an Axoprobe-1A amplifier (Molecular Devices Corp., Sunnyvale, CA, USA), AC-coupled and amplified a further 100× (NL-106 AC-DC Amp: Digitimer Ltd., Welwyn Garden City, UK), before being band-pass filtered between 0.3 and 5 kHz (NL125: Digitimer). All biopotentials were digitized on-line with a PC running Spike2 acquisition and analysis software (version 5; Cambridge Electronic Design, Cambridge, UK). Extracellular recordings of multi-unit activity in the PPN were made using "silicon probes" (model number 1 cm 100–400; NeuroNexus Technologies, Ann Arbor, MI, USA). Each probe had 16 recording contacts arranged in a single vertical plane, with a contact separation of 100 μm. Each contact had an impedance of 0.9–1.3 MΩ (measured at 1000 Hz) and an area of ~400 μm^2. Monopolar signals recorded using the probes were referenced against a screw implanted in the skull above the contralateral cerebellar hemisphere. Probes were advanced into the brain under stereotaxic control (Paxinos and Watson, 1986), at an angle of 15° to the vertical to avoid prominent blood vessels. Probes were advanced slowly using a zero-drift micromanipulator (1760–61; David Kopf Instruments), and large blood vessels (greater than ~50 μm diameter) lying on the cortical surface were avoided. This approach ensured that dimpling of the cortex was avoided and that no gross deformation or bending of the probe occurred. Extracellular signals from the silicon probe were amplified (1000–2000×) and low-pass filtered (0–6000 Hz) using computer-controlled differential amplifiers (lynx-8; Neuralynx, Tucson, AZ, USA). The ECoG and probe signals were each sampled at 17.5 kHz. The ECG and respiration signals were sampled at 400 and 64 Hz, respectively. All biopotentials were digitized on-line using a Power1401 analog-to-digital converter (Cambridge Electronic Design, Cambridge, UK) and a personal computer running Spike2

acquisition and analysis software. Recording locations were verified using histological procedures.

Activity was recorded, firstly, during SWA, which accompanies deep anesthesia and is similar to activity observed during natural (non-REM) sleep, and secondly, during episodes of spontaneous or sensory-evoked "global activation," which contain patterns of activity that are more analogous to those observed during the awake, behaving state (see review by Steriade, 2000). Sensory stimulation and subsequent global activation were elicited by a standard calibrated pinch of the hind paw delivering a standard pressure of 183 g/mm^2. The animals did not respond overtly to the pinch. There was a wide variability within individual recordings and between different animals regarding the changes following the pinches and the duration of the effects. Thus, following the initial effect of the pinch (obliteration of the cortical slow oscillations), fast-frequency low-amplitude activity was observed in the ECoG for variable periods of time. In most cases, it was eventually replaced by a mixture of many intermediate frequencies, eventually leading back to slow oscillations. On some occasions, additional doses of anesthetics had to be administered in order to force the system to return to SWA.

Juxtacellular labeling of single neurons

Following the electrophysiological recordings, neurons were labeled with neurobiotin in order to verify their locations and identify their neurochemical and morphological properties (Pinault, 1996). A microiontophoretic current was applied (1–10 nA positive current, 200 ms duration, 50% duty cycle) while the electrode was advanced slowly towards the neuron. The optimal position of the electrode was identified when the firing pattern of the neuron was robustly modulated by the current injection. The modulation of the neuronal firing was maintained for at least 2 min in order to obtain reliable labeling. Then the neurobiotin was allowed to transport along neuronal processes for between 5 and 12 h. Following the diffusion time, the animals were given a lethal dose of ketamine (150 mg/kg) and intracardially perfused with 0.05 M phosphate buffered saline (PBS), pH 7.4, followed by 300 ml of 4% w/v paraformaldehyde and 0.1% w/v glutaraldehyde in phosphate buffer (0.1 M pH 7.4). Brains were stored in PBS at 4 °C until sectioning.

Histochemistry and immunohistochemistry

Brains were sectioned at 50 μm in the parasagittal plane on a vibratome and the neurochemical identity of juxtacellularly-labeled PPN neurons was verified using standard immunofluorescence and histofluorescence techniques. In order to identify the neurochemical profile of the labeled neurons, the neurobiotin was revealed by incubation with CY3-conjugated streptavidin (1:1000; Jackson ImmunoResearch Laboratories, Inc., USA) in PBS containing 0.3% v/v Triton X-100. For neurons destined for electron microscopy, the Triton X-100 was omitted but the sections were freeze-thawed prior to processing (see below). The presence of choline acetyltransferase (ChAT), the synthetic enzyme for acetylcholine, was revealed by incubation in goat anti-ChAT antibodies (1:500, Chemicon, USA), followed by Alexa 488-conjugated donkey anti-goat antibodies (1:1000, Jackson ImmunoResearch Laboratories, Inc.). Sections were then mounted on slides for viewing with a conventional epifluorescence microscope (DMRB: Leica Microsystems

GmbH, Wetzlar, Germany) or a laser-scanning confocal fluorescence microscope (LSM510: Karl Zeiss AG, Oberkochen, Germany). Only ChAT-negative neurons were analyzed in detail here (ChAT-positive neurobiotin-labeled neurons served as positive controls in the same series). The control ChAT labeling was evaluated by the presence of positive immunoreactivity in the cytoplasm of PPN neurons (consistent with previous reports on the number and distribution of cholinergic neurons; Mena-Segovia et al., 2009) at the same focal planes of intermingled neurobiotin-labeled ChAT-negative neurons. Only those non-cholinergic neurons located within the cholinergic borders of the PPN (either in the same section or adjacent sections) were included in this study.

Following neurochemical identification, standard histochemical techniques were used to visualize cells with a permanent peroxidase reaction product for light and electron microscopic analyses. Sections used only for light microscopy were washed in PBS and incubated overnight in avidin-biotin-peroxidase complex (ABC Elite; 1:100; Vector Laboratories) in PBS containing 0.3% v/v Triton X-100. Following a series of washes in Tris buffer (0.05 M, pH 8.0), the sections were incubated in hydrogen peroxide (0.002% w/v; Sigma, UK) and diaminobenzidine tetrahydrochloride (0.025% w/v; Sigma) dissolved in Tris buffer. Sections for electron microscopy were first equilibrated in cryoprotectant solution (0.05 M PB, pH 7.4, 25% sucrose, 10% glycerol) overnight before being freeze-thawed by freezing isopentane (VWR International Ltd., Poole, England) cooled in liquid nitrogen and thawing in PBS. The sections were washed and then revealed as for light microscopy. After revealing the neurobiotin, sections were postfixed with 1% w/v osmium tetroxide in PB (Oxkem, Oxford, UK) for 25 min and then dehydrated through a graded series of alcohol solutions and 1% w/v uranyl acetate (TAAB Laboratories, Berkshire, UK) in the 70% ethanol solution. Following dehydration, sections were treated with propylene oxide (Sigma) and placed in resin overnight (durcupan ACM; Fluka, Dorset, UK). Finally, the sections were mounted on slides and placed in an oven at 60 °C for 48 h.

Three-dimensional reconstruction of single neurons

The somatodendritic and axonal arborizations of neurobiotin-labeled, non-cholinergic PPN neurons were reconstructed from successive serial sections (50 μm) using a 63× objective, and were digitized using Neurolucida software (MicroBrightField, Williston, USA).

Area segmentation and location of neurons

In order to define the specific location of each labeled neuron across the rostrocaudal axis of the PPN, the area that contains the PPN was segmented with the aid of external landmarks, as described before (Mena-Segovia et al., 2009). Using Neurolucida software, concentric circles originating in the center of the substantia nigra pars reticulata (SNR) with increasing radii (in steps of 300 μm) were overlapped onto parasagittal sections containing one or more of the labeled PPN neurons. The PPN was contained in up to 10 concentric segments, and its perimeter was defined by ChAT-positive neurons. Segments 1–5 were considered rostral PPN and segments 6–10 were considered caudal PPN.

Europe PMC Funders Author Manuscripts

Criteria for inclusion

We obtained 102 neurons recorded and labeled by the juxtacellular method. The majority of those neurons were discarded on the basis of the depth of the anesthesia, the absence of cortical slow oscillations or their location outside the cholinergic boundaries of the PPN.

Neurons in the present study were mainly selected and categorized on the basis of their lack of immunoreactivity for ChAT. In cases when neurons were obtained from multi-unit (silicon probe) recordings, or when the immunohistochemical identity of the labeled neurons could not be confirmed, they were assigned to a group on the basis of their physiological properties (firing rate and coefficient of variation). Thus, non-labeled neurons that did not show a preferential firing for any of the phases of the neocortical slow oscillations (lack of meaningful correlations using phase histograms, data not shown; see Mena-Segovia et al., 2008) were included in our analysis.

Electrophysiological data and statistical analysis

Electrophysiological data were digitized using a Power 1401 Analog-Digital converter (Cambridge Electronic Design) and analyzed with a PC running Spike2 software (Cambridge Electronic Design). Spike trains composed of 100 spikes during coincident SWA activity in the ECoG were isolated and used for the criteria of inclusion and standard statistical analysis, including extracellular action potential waveform, spontaneous firing rate (Hz) and the coefficient of variation of spiking (CV, a standard measure of regularity). In cases when the 100 spikes criterion could not be satisfied because of the slow firing frequency of the neuron (as in the case of quiescent neurons), recordings were kept as long as possible (sometimes up to 15 min). To quantify the responses of PPN neurons to the brain state transitions, spike trains were analyzed for differences in the firing rate before, during and after the sensory stimulation (pinch), as described before (Brown et al., 2009). Briefly, a baseline of spontaneous unit activity (mean firing rate) was established for the 30 s of activity immediately prior to the onset of the pinch. This baseline was compared to the activity both during, and 15 s immediately after, the pinch. The mean firing rate and standard deviation (SD) of activity during the baseline period were calculated. Firing rate was plotted against time (500 ms bins) and the number of bins above and below 2 SDs from the baseline mean rate were calculated. A neuron was defined as significantly inhibited or excited by a pinch stimulus if two consecutive histogram bins within the 15 s stimulus period lay outside 2 SDs from the baseline mean rate. The figures show longer traces to better represent the dynamics of the neuronal firing before and after the pinch.

Action potentials were measured for their biphasic duration from the beginning of the positive deflection to the lowest point of the negative trough (Brown et al., 2009).

The Wilcoxon signed-rank test was used to compare paired data. The significance level for all tests was taken to be $P<0.05$. Data are expressed as mean±standard error of the mean (SEM).

Electron microscopy

Following light microscopic analysis, regions of tissue containing local axon collaterals of juxtacellularly labeled PPN neurons were re-embedded and re-sectioned at ~50 nm using a Leica EM UC6 ultramicrotome (Leica Microsystems). These sections were collected onto Pioloform-coated, single-slot grids (Agar Scientific, Stansted, UK), stained with lead citrate and examined in a Philips CM100 or CM10 electron microscope. Electron micrographs of labeled axon collaterals were captured for each section using a Gatan multiscan CCD camera (Gatan, Abingdon, UK) at final magnifications ranging from 54,000×–138,000× and these were then examined for evidence of synaptic contacts formed with other PPN structures. Asymmetrical and symmetrical synapses formed by labeled axon collaterals were defined by the presence of four criteria: presynaptic vesicle accumulation, membrane specializations, a widened synaptic cleft and cleft material. Synapses were confirmed by examination in serial ultrathin sections. Images of synapses were adjusted for contrast and brightness using Adobe Photoshop (Version CS3, Adobe Systems Incorporated, San Jose, CA, USA).

RESULTS

Neocortical activity and brain state transitions

Urethane anesthesia typically produced SWA characterized by a stable slow oscillation in the neocortex that bears a close resemblance to the activity observed during the deeper stages of natural slow-wave (non-REM) sleep in mammals. These slow oscillations were defined by their large amplitude (>400 μV) and low frequency (~1 Hz). The portions of the slow oscillation supporting fast oscillations (i.e., spindles and gamma frequency oscillations) will be referred to hereafter as the “active component” (neocortical up-state). The portions during which high-frequency oscillations are weakest, or absent, will thus be referred to as the “inactive component” (neocortical down-state). SWA was spontaneously interspersed with periods of neocortical activation (also referred to as the activated state), defined by a progressive disappearance of slow oscillations that were replaced by a sustained (>3 s) period of low amplitude (<200 μV) and fast frequency (>5 Hz) heterogeneous activity. Neocortical activation could also be abruptly induced by sensory stimulation (foot pinch). The response time of the cortex to switch from SWA to an activated state following sensory stimulation varied between animals and conditions, and was particularly dependent on the depth of anesthesia.

Neuronal diversity within the population of non-cholinergic PPN neurons

We recorded the spontaneous action potential discharges of individual PPN neurons during neocortical slow oscillations and during the transition to an activated state (induced by sensory stimulation), and we then labeled the neurons using the juxtacellular method. Neurons in this study (n=17) were categorized on the basis of their electrophysiological properties and lack of immunoreactivity for ChAT, or their electrophysiological properties alone. Some non-identified neurons, whose chemical phenotype could not be characterized but whose firing was uncorrelated to the neocortical slow oscillations, and those obtained from multi-unit recordings, were assigned to a particular group on the basis of their electrophysiological properties (see criteria for inclusion, in methods). We observed a large

variability in the physiological properties of these non-cholinergic neurons, in terms of their firing rates and firing patterns, and their activity fluctuations between global brain states. These properties were distinct from the properties of those non-cholinergic neurons that have been previously described and are strongly correlated to neocortical activity (Mena-Segovia et al., 2008). In contrast to the robust increase in the firing rate of cholinergic neurons during transitions to neocortical activation (see Mena-Segovia et al., 2008), non-cholinergic neurons showed a wide variability in the types and magnitudes of their responses (i.e. excitation, inhibition or no response). Because SWA tends to stereotype and group the activity of functionally distinct classes of neurons, as previously observed in the PPN and elsewhere (e.g. Mena-Segovia et al., 2008; Ros et al., 2009), we grouped non-cholinergic neurons into three different categories according to their firing properties during SWA, albeit with a small sample size: quiescent neurons, tonic firing neurons and irregular firing neurons (Fig. 1A). After neurochemical characterization by immunofluorescence, the recorded PPN neurons were processed to reveal the neuronal marker, neurobiotin, with a permanent peroxidase reaction product that enabled us to examine and reconstruct their dendrites and axonal arbors. Labeled neurons from the tonic firing and irregular firing subgroups were found intermingled across the entire rostro-caudal extent of the PPN. In contrast, quiescent neurons were only concentrated in the caudal part of the nucleus (Fig. 1B). The physiological and morphological properties of these three types of neurons are summarized in Table 1.

Quiescent neurons—Three identified non-cholinergic neurons (Fig. 2A–D) were characterized by a very slow firing rate during robust SWA. Two neurons whose chemical phenotype was not characterized showed a similar firing pattern during SWA (i.e. almost silent) were included in this category. All neurons in this group were located in the caudal PPN (Fig. 1B). Their firing rate during SWA ranged from 0.01 to 0.6 Hz (mean 0.27±0.1 Hz, n=5; Fig. 2), and they had a mean CV of 1.13±0.13 (SEM). Quiescent neurons had distinct axonal arborizations that were different from all other types of neurons (see Suppl. Fig. 1). Three neurons gave rise to an axon that traveled caudally from the cell body before looping and ascending rostrally, and sometimes branching, towards the basal ganglia via dorsal and ventral pathways (Fig. 2A; Suppl. Fig. 1), innervating the subthalamic nucleus, substantia nigra *pars reticulata* and substantia nigra *pars compacta*. The reconstruction, polar histograms and Scholl analyses show that the axon traveled rostrally in the sagittal plane (Fig. 2E) and that the highly-branched dendrites were organized in a radial manner (Fig. 2F, G). No descending axon collaterals were observed in this group. The axon of the neuron depicted in Fig. 2 produced varicosities both locally (n=11) and in its basal ganglia target regions (n=41), some of which were confirmed by electron microscopy to give rise to asymmetric synapses (see Fig. 7). The firing of quiescent neurons was not correlated with the neocortical slow oscillation (Fig. 2I). Following sensory stimulation, the three neurons that were identified as non-cholinergic by immunolabeling responded robustly by showing a prolonged increase in their firing rate (Fig. 2J). Of the two remaining neurons, one decreased its firing rate whereas the other showed neither an increase nor a decrease in firing rate following the stimulation.

Tonic firing neurons—Neurons in this category were homogeneous and primarily characterized by a fast and regular firing rate during SWA, ranging from 9 to 24 Hz (mean 19.14±3.54; *n*=4; Fig. 3), with a CV typically less than 0.3 (mean 0.27±0.01), and a short action potential duration (mean 0.69±0.06 ms; Fig. 3G). Two of these neurons were identified as non-cholinergic following a negative immunoreaction for ChAT (Fig. 3A–C); two neurons that were not characterized by immunofluorescence but that fired tonically during SWA were also included in this category. Tonic firing neurons showed a different pattern of axonal projections, typically emitting a single branch directed caudally and then turning and traveling rostrally along the superior cerebellar peduncle (scp) fibers (Fig. 3A, D; Suppl. Fig. 2) without giving rise to local arborizations. Axons mainly traveled in the rostro-caudal plane rather than the mediolateral plane; no descending collaterals were observed in this group. The polar histograms and the Scholl analysis show that the axon had a low level of tortuosity (Fig. 3D, F) and that dendrites were sparse and radial (Fig. 3E). Tonic firing neurons did not show any preferential firing during any phase of the neocortical slow oscillation (Fig. 3H). Three out of the four neurons in this group did not significantly change their firing rate following sensory stimulation (Fig. 3J), the fourth showed an increased firing rate.

Irregular firing neurons—Neurons that did not fit in any of the previous two categories and that did not show a strong correlation with the neocortical slow oscillations were grouped as “irregular firing neurons.” For this reason, neurons in this group were highly heterogeneous in terms of their morphological and physiological properties. Four of the neurons in this group were confirmed as non-cholinergic following a negative immunoreaction for ChAT (Figs. 4A–C and 5A–D), and four additional non-labeled neurons were included in this category on the basis of their uncorrelated firing with neocortical slow oscillations. Thus, irregular firing neurons were characterized by a slow and irregular firing rate during SWA, ranging from 1.4 to 4.4 Hz (mean 2.62±0.27; *n*=7; Figs. 4 and 5), and a CV ranging from 0.3 to 1.8 (mean 0.71±0.15). One non-cholinergic neuron was not electrophysiologically evaluated. Within this category of neurons, the change in firing rate following the sensory stimulation was highly heterogeneous, ranging from moderate to strong responses and included excitation, inhibition or no change (see Table 1, Figs. 4I and 5J). Thus, neurons increased (*n*=2), decreased (*n*=1), or had no change (*n*=2) in their firing rate following sensory stimulation, and two neurons had a bimodal response, showing a short-latency increase followed by a long-lasting reduction of several seconds after the off-set of the pinch.

Typically, the dendrites of these neurons were long (mean total dendritic length of 3534 μm) and bipolar, arising from elongated oval somata (Fig. 4A, E). In contrast to quiescent neurons that projected to nuclei of the basal ganglia, irregular neurons had axons that showed single distinct axonal trajectories, such as dorsally ascending axons (Fig. 4; see also Suppl. Fig. 3) or descending-only axons (Fig. 5; see also Suppl. Fig. 4). In this first subcategory, the axon of these neurons travelled dorsally towards the tectum, in the direction of the cholinergic axons (seen in ChAT-immunolabeled sections) travelling towards the thalamus (Fig. 4D). These neurons tended to have a mild and brief response to the sensory stimulation or no significant change in their firing rate (Fig. 4I).

We also observed in this group two neurons with descending axons (Fig. 5A, E; Suppl. Fig. 4) that did not give rise to any local boutons within the PPN. One of them showed an exclusively descending trajectory (Fig. 5A). Polar histograms demonstrate a bipolar and branching dendritic arborization (Fig. 5F). The firing of these neurons was extremely heterogeneous with spontaneous periods of silence alternated with stereotyped activity and sporadic coupling to the slow oscillations but without a clear sustained relationship (Fig. 5I). Both neurons showed a decrease in the firing rate during the pinch, which was linked to the sensory stimulation rather than to the neocortical activation (Fig. 5J).

Simultaneous multi-unit recordings

In order to determine whether these three types of firing in PPN neurons occur simultaneously, we recorded PPN multi-unit activity in three animals using high-density electrodes under the same anesthetic conditions. During slow-wave activity, we observed all patterns of activity in PPN neurons described so far: neurons coupled to the cortical slow oscillations (as described in Mena-Segovia et al., 2008) and neurons showing quiescent, tonic or irregular firing (Fig. 6). Thus, quiescent neurons showed a very slow firing rate and no coupling to any phase of the slow oscillations, tonic firing neurons showed a fast firing rate and no coupling to the slow oscillations, and irregular firing neurons showed a wide variation in their firing rate and pattern, and were predominantly independent of slow oscillations. All three types of firing patterns were observed to occur simultaneously, suggesting that such properties are non-dynamic attributes of the neuronal subtypes observed from the single cell labeling experiments.

Local connectivity

From the 17 juxtacellularly labeled neurons included in this study, 13 were labeled strongly and allowed us to trace the axon and identify putative connections. Four of these possessed local varicosities within the PPN (mean number of boutons: 22±4) and were identified as non-cholinergic. Two of the neurons were quiescent neurons and two were irregular firing neurons; we did not observe varicosities in the local axon collaterals of tonic firing neurons. All of them were located in the caudal PPN, and three out of four increased their firing rate following sensory stimulation (one neuron was not evaluated).

The local axon collaterals of non-cholinergic neurons typically showed a loop that initially travels in a caudal direction, following the fibers of the scp, before turning back on itself and travelling rostrally towards the SNR. We examined the axons of two juxtacellularly-labeled PPN neurons in the electron microscope for evidence of intrinsic connectivity in the PPN. The axon of one of these neurons was myelinated (0.25–0.80 μm in diameter), it contained mitochondria along its length and gave rise to smaller diameter unmyelinated collaterals (Fig. 7A, C) that formed large boutons containing multiple mitochondria and forming asymmetrical synaptic contacts with dendritic shafts (0.5–2.90 μm in diameter; Fig. 7A, B, D).

The axon of the second neuron was unmyelinated (0.1–0.35 μm) and gave rise to varicosities (approximately 0.50 μm in diameter) that contained 1–2 small mitochondria, but were not

seen to form local synaptic specializations. This axon was seen to form asymmetrical synaptic contacts in the subthalamic nucleus.

DISCUSSION

The present findings support the notion of the PPN as a highly heterogeneous structure in terms of both the morphological and physiological properties of different populations of neurons. We labeled non-cholinergic neurons after recording them in parallel with neocortical activity and grouped them into three categories: quiescent neurons, tonic firing neurons and irregular firing neurons. In addition to differences in their firing rate during neocortical slow oscillations, these groups were also distinguished on the basis of their response to cortical brain state transitions, the trajectory of their axon and their local connectivity. The large variability observed among subsets of non-cholinergic neurons with distinct firing properties and their interaction as part of an integrated local network may therefore underlie the diversity of behavioral processes in which the PPN is involved.

Coupling with neocortical activity

During non-REM sleep and urethane anesthesia, activity in the neocortex is characterized by synchronized oscillations of neurons and networks at a frequency of about 1 Hz (~0.8 Hz; Steriade et al., 1993). Slow network oscillations impose spatially and temporally coherent activity both within, and between, the neocortex and subcortical structures (Crunelli and Hughes, 2010; Ros et al., 2009; Volgushev et al., 2006). We and others have previously shown that the activity in the PPN during SWA is highly synchronized with neocortical slow oscillations under different anesthetic regimes (Aravamuthan et al., 2008; Mena-Segovia et al., 2008). Thus, we have shown that the discharge of identified neighboring cholinergic neurons and a subpopulation of non-cholinergic neurons are temporally coupled to distinct phases of neocortical slow oscillations, suggesting a role in the modulation of the phasic events that encompass the slow oscillations (Mena-Segovia et al., 2008). Here, we show that the firing of three distinct subtypes of non-cholinergic neurons display variable levels of coupling to neocortical slow oscillations. Quiescent neurons fire sparsely and tonic firing neurons maintain a fast regular discharge, but neither exhibit a preference for any phase of the slow oscillation. In contrast, some of the irregular firing neurons show a sporadic correlation albeit weak. These findings suggest that different populations of PPN neurons are differentially modulated by their afferents during SWA and show that there is not a complete entrainment of the PPN by the neocortex during slow oscillations.

The PPN has long been considered part of a large brainstem network that is able to modulate brain state transitions. Classic studies by Moruzzi and Magoun (1949) and Steriade and colleagues (1991) have shown that activation of the brainstem leads to transitions from SWA to an activated state that is characterized by fast-frequency low-amplitude oscillations, typical of wakefulness (or arousal) and REM sleep. Furthermore, extracellular recordings from the PPN have shown an overall reduction in its neuronal activity during SWA and an overall increase during the activated state (Steriade et al., 1990; Datta and Siwek, 2002; Balatoni and Detari, 2003). However, using the pinch-induced cortical activation model, our results show a large variability in the response of neurochemically- and morphologically-

Europe PMC Funders Author Manuscripts

identified PPN neurons during the transition towards activation of the cortex. Cholinergic neurons exhibit a robust increase in their firing rate following sensory-induced neocortical activation (which is in good agreement with the prediction of the RAS model; for example Steriade and colleagues, 1991 (Curro Dossi et al., 1991) prevented cortical activation by blocking cholinergic transmission). However, non-cholinergic neurons follow different patterns: they show activation (60% of quiescent neurons and 57% of irregular firing neurons), inhibition (20% of quiescent neurons and 14% of irregular firing neurons) or no change in their firing rate (75% of tonic firing neurons and 29% of irregular firing neurons) during sensory-induced neocortical activation. Interestingly, the discharge of some of the quiescent neurons during neocortical slow oscillations could have met the proposed *SWA-silent* criteria of presumed cholinergic PPN neuron firing, as typically described elsewhere (for a comprehensive review see Steriade and McCarley, 2005), therefore suggesting a contribution of this subtype of non-cholinergic neurons to the regulation of the sleep-wake cycle.

Our findings demonstrate that PPN neurons are not uniformly excited in response to a transition from SWA to an activated state but rather, they show a highly heterogeneous response associated with distinct neuronal subpopulations. Of particular note are those neurons that decreased their firing following the stimulation paradigm designed to produce neocortical activation. Considering the neurochemical heterogeneity and the large number of GABAergic neurons in the PPN, it is likely that some of these neurons generate a local inhibitory modulation.

Classification of neurons in the PPN

There have been past efforts to classify neurons in the PPN, most of them in terms of their physiological properties *in vitro* (Leonard and Llinas, 1994; Takakusaki et al., 1996, 1997). Here we provide the first neurochemical and morphological correlation with the physiological properties of non-cholinergic PPN neurons recorded *in vivo*. For the purpose of classification, we used their firing patterns during the neocortical slow oscillations as a standard temporal reference, which has proven to be useful for classifying other neuronal subpopulations in the PPN (Mena-Segovia et al., 2008). This approach led us to identify three categories of non-cholinergic neurons (quiescent, tonic firing and irregular firing neurons) that differ in their firing during SWA, their response to brain state transitions and their pattern of connectivity. Because the level of anesthesia tends to have an influence on the firing frequency and responses, only those recordings in which the slow oscillations were obliterated after the sensory stimulation (as a measure for the depth of anesthesia) were considered for the physiological analysis (16 out of 17). One neuron was analyzed only for its anatomical properties.

Of the three categories of non-cholinergic neurons, the group of irregular firing neurons was the most heterogeneous. Since no other criteria could group them reliably, we included them in a single category based on their lack of similarities to any of the other categories (either the ones described here or those from a previous report; Mena-Segovia et al., 2008). Therefore, considering also the small sample size, it is possible that some of the neurons in the “irregular firing” group may have to be re-classified in the future when more information

on the properties of each neuronal subtype in the PPN becomes available. Nevertheless, such heterogeneity could give important clues on the functional circuits in which they are integrated. Since their firing rate and patterns during brain state transitions ranged across all possible responses, it is possible that irregular firing neurons may share similar modulatory afferents during SWA but belong to a different functional circuit involved in the modulation of brain states.

Connectivity of non-cholinergic neurons

Single-cell labeling showed that some non-cholinergic PPN neurons produce local axon varicosities, some of which were identified as making synaptic contacts within the PPN. Although there was some variability in the number of local varicosities, and the numbers were not as large as those for cholinergic neurons (Mena-Segovia et al., 2008), this evidence suggests a role for non-cholinergic neurons in the structuring of local activity. Besides the cholinergic neurons, two other main populations have been described in the PPN: the glutamatergic and the GABAergic neurons (Ford et al., 1995; Mena-Segovia et al., 2009; Wang and Morales, 2009). It is thus likely that most of our recorded and labeled neurons would utilize either glutamate or GABA as their neurotransmitter. The difficulty in identifying the neurochemical phenotype of these neurons resides in the inconsistency of the results given by conventional immunohistochemical techniques for identifying glutamatergic or GABAergic neurons in the PPN. Nevertheless, ultrastructural features may help to determine the neurochemical nature of PPN neurons. The two neurons examined formed asymmetric synaptic contacts (one of them local, the other in the basal ganglia), suggesting an excitatory nature, most likely glutamatergic (Bevan and Bolam, 1995). Thus, these findings provide the first evidence that excitatory non-cholinergic (i.e. putative glutamatergic) synaptic contacts contribute to the local network. The neurons giving rise to those boutons increased their firing rate during the transition from SWA to an activated state. Since these neurons are likely to be glutamatergic, it suggests a role for glutamatergic neurons in the activation of the PPN and the modulation of its targets (e.g. basal ganglia).

The contribution to the local connectivity of GABAergic neurons in the PPN still remains to be determined. Here we speculate that tonic firing neurons are GABAergic neurons. They have a typical short action potential-duration and a fast firing rate, characteristics that are comparable with GABAergic neurons elsewhere in the brain. In addition, they have a small soma size, comparable to that of identified GABAergic neurons following *in situ* hybridization in the PPN (Mena-Segovia et al., 2009). We did not observe any varicosities arising from the axons of these tonic-firing neurons, which suggests that they do not have a role in the local connectivity, although the possibility of dendro-dendritic synapses cannot be ruled out (Pinault et al., 1997). Thus, they may be projection neurons, which have been described previously (Bevan and Bolam, 1995; Ford et al., 1995; Charara et al., 1996). The presence of this subtype of neurons in the PPN, whose firing is independent of the cortex, raises the question as to whether they play a different role in the functions of the PPN and whether that role is reflected by their targets in other neural systems. Also, their lack of response to global state transitions, which are presumably driven by cholinergic neurons, implies that they occupy a different position in the local network in the PPN.

Europe PMC Funders Author Manuscripts

Functional implications

The present study, together with our earlier study, emphasizes the wide diversity in the neuronal types that comprise the PPN. The varied structures served by the PPN, via numerous pathways, are crucially involved in the control of movement and sensorimotor coordination (basal ganglia), sleep-wake mechanisms and arousal (thalamus), and locomotion and autonomic functions (brainstem and spinal cord). The finding that non-cholinergic PPN neurons are heterogeneous with respect to their firing rates and patterns, that they can change their activity during sensory-evoked neocortical activation, taken together with anatomical findings that non-cholinergic neurons can simultaneously influence the local activity as well as the activity of several targets, underlines the potentially important roles played by the non-cholinergic component of the PPN. Thus, these data call for a reappraisal of the role and relative importance of non-cholinergic neurons in information processing associated to the overall network properties of the PPN.

Supplementary Material

Refer to Web version on PubMed Central for supplementary material.

Acknowledgments

This work was supported by the Medical Research Council UK, the Parkinson's UK (grant no. 4049) and the Parkinson's Disease Foundation. We thank B. Micklem, E. Norman, C. Francis and K. Whitworth for their technical assistance.

Abbreviations

ChAT	choline acetyltransferase
CV	coefficient of variation
ECoG	electrocorticogram
PBS	phosphate buffered saline
PPN	pedunculopontine nucleus
RAS	reticular activating system
REM	rapid eye movement
scp	superior cerebellar peduncle
SNR	substantia nigra pars reticulata
SWA	slow-wave activity

REFERENCES

Ainge JA, Keating GL, Latimer MP, Winn P. The pedunculopontine tegmental nucleus and responding for sucrose reward. Behav Neurosci. 2006; 120:563–570. [PubMed: 16768608]

Aravamuthan BR, Bergstrom DA, French RA, Taylor JJ, Parr-Brownlie LC, Walters JR. Altered neuronal activity relationships between the pedunculopontine nucleus and motor cortex in a rodent model of Parkinson's disease. Exp Neurol. 2008; 213:268–280. [PubMed: 18601924]

Balatoni B, Detari L. EEG related neuronal activity in the pedunculopontine tegmental nucleus of urethane anaesthetized rats. Brain Res. 2003; 959:304–311. [PubMed: 12493619]

Bevan MD, Bolam JP. Cholinergic, GABAergic, and glutamate-enriched inputs from the mesopontine tegmentum to the subthalamic nucleus in the rat. J Neurosci. 1995; 15:7105–7120. [PubMed: 7472465]

Brown MT, Henny P, Bolam JP, Magill PJ. Activity of neurochemically heterogeneous dopaminergic neurons in the substantia nigra during spontaneous and driven changes in brain state. J Neurosci. 2009; 29:2915–2925. [PubMed: 19261887]

Charara A, Smith Y, Parent A. Glutamatergic inputs from the pedunculopontine nucleus to midbrain dopaminergic neurons in primates: phaseolus vulgaris-leucoagglutinin anterograde labeling combined with postembedding glutamate and GABA immunohistochemistry. J Comp Neurol. 1996; 364:254–266. [PubMed: 8788248]

Corrigall WA, Coen KM, Zhang J, Adamson L. Pharmacological manipulations of the pedunculopontine tegmental nucleus in the rat reduce self-administration of both nicotine and cocaine. Psychopharmacology. 2002; 160:198–205. [PubMed: 11875638]

Crunelli V, Hughes SW. The slow (<1 Hz) rhythm of non-REM sleep: a dialogue between three cardinal oscillators. Nat Neurosci. 2010; 13:9–17. [PubMed: 19966841]

Curro Dossi R, Pare D, Steriade M. Short-lasting nicotinic and long-lasting muscarinic depolarizing responses of thalamocortical neurons to stimulation of mesopontine cholinergic nuclei. J Neurophysiol. 1991; 65:393–406. [PubMed: 2051187]

Curto C, Sakata S, Marguet S, Itskov V, Harris KD. A simple model of cortical dynamics explains variability and state dependence of sensory responses in urethane-anesthetized auditory cortex. J Neurosci. 2009; 29:10600–10612. [PubMed: 19710313]

Datta S, Siwek DF. Single cell activity patterns of pedunculopontine tegmentum neurons across the sleep-wake cycle in the freely moving rats. J Neurosci Res. 2002; 70:611–621. [PubMed: 12404515]

Donoghue JP, Wise SP. The motor cortex of the rat: cytoarchitecture and microstimulation mapping. J Comp Neurol. 1982; 212:76–88. [PubMed: 6294151]

Ford B, Holmes CJ, Mainville L, Jones BE. GABAergic neurons in the rat pontomesencephalic tegmentum: codistribution with cholinergic and other tegmental neurons projecting to the posterior lateral hypothalamus. J Comp Neurol. 1995; 363:177–196. [PubMed: 8642069]

Garcia-Rill E, Houser CR, Skinner RD, Smith W, Woodward DJ. Locomotion-inducing sites in the vicinity of the pedunculopontine nucleus. Brain Res Bull. 1987; 18:731–738. [PubMed: 3304544]

Good CH, Lupica CR. Properties of distinct ventral tegmental area synapses activated via pedunculopontine or ventral tegmental area stimulation *in vitro*. J Physiol. 2009; 587:1233–1247. [PubMed: 19188251]

Heinmiller A, Ting-A-Kee R, Vargas-Perez H, Yeh A, van der Kooy D. Tegmental pedunculopontine glutamate and GABA-B synapses mediate morphine reward. Behav Neurosci. 2009; 123:145–155. [PubMed: 19170439]

Jones BE. From waking to sleeping: neuronal and chemical substrates. Trends Pharmacol Sci. 2005; 26:578–586. [PubMed: 16183137]

Leonard CS, Llinas R. Serotonergic and cholinergic inhibition of mesopontine cholinergic neurons controlling REM sleep: an *in vitro* electrophysiological study. Neuroscience. 1994; 59:309–330. [PubMed: 8008195]

Magill PJ, Sharott A, Bolam JP, Brown P. Brain state-dependency of coherent oscillatory activity in the cerebral cortex and basal ganglia of the rat. J Neurophysiol. 2004; 92:2122–2136. [PubMed: 15175372]

Maskos U. The cholinergic mesopontine tegmentum is a relatively neglected nicotinic master modulator of the dopaminergic system: relevance to drugs of abuse and pathology. Br J Pharmacol. 2008; 153(Suppl 1):S438–S445. [PubMed: 18223661]

McCarley RW. Neurobiology of REM and NREM sleep. Sleep Med. 2007; 8:302–330. [PubMed: 17468046]

Mena-Segovia J, Micklem BR, Nair-Roberts RG, Ungless MA, Bolam JP. GABAergic neuron distribution in the pedunculopontine nucleus defines functional subterritories. J Comp Neurol. 2009; 515:397–408. [PubMed: 19459217]

Mena-Segovia J, Sims HM, Magill PJ, Bolam JP. Cholinergic brainstem neurons modulate cortical gamma activity during slow oscillations. J Physiol. 2008; 586:2947–2960. [PubMed: 18440991]

Moruzzi G, Magoun HW. Brain stem reticular formation and activation of the EEG. Electroencephalogr Clin Neurophysiol. 1949; 1:455–473. [PubMed: 18421835]

Nandi D, Stein JF, Aziz TZ. Exploration of the role of the upper brainstem in motor control. Stereotact Funct Neurosurg. 2002; 78:158–167. [PubMed: 12652040]

Okada K, Toyama K, Inoue Y, Isa T, Kobayashi Y. Different pedunculopontine tegmental neurons signal predicted and actual task rewards. J Neurosci. 2009; 29:4858–4870. [PubMed: 19369554]

Paxinos, G.; Watson, C. The rat brain in stereotaxic coordinates. Academic Press; San Diego, CA: 1986.

Pinault D. A novel single-cell staining procedure performed *in vivo* under electrophysiological control: morpho-functional features of juxtacellularly labeled thalamic cells and other central neurons with biocytin or Neurobiotin. J Neurosci Methods. 1996; 65:113–136. [PubMed: 8740589]

Pinault D, Smith Y, Deschenes M. Dendrodendritic and axoaxonic synapses in the thalamic reticular nucleus of the adult rat. J Neurosci. 1997; 17:3215–3233. [PubMed: 9096155]

Ros H, Sachdev RN, Yu Y, Sestan N, McCormick DA. Neocortical networks entrain neuronal circuits in cerebellar cortex. J Neurosci. 2009; 29:10309–10320. [PubMed: 19692605]

Saper CB, Scammell TE, Lu J. Hypothalamic regulation of sleep and circadian rhythms. Nature. 2005; 437:1257–1263. [PubMed: 16251950]

Steriade M. Corticothalamic resonance, states of vigilance and mentation. Neuroscience. 2000; 101:243–276. [PubMed: 11074149]

Steriade M, Datta S, Pare D, Oakson G, Curro Dossi RC. Neuronal activities in brain-stem cholinergic nuclei related to tonic activation processes in thalamocortical systems. J Neurosci. 1990; 10:2541–2559. [PubMed: 2388079]

Steriade M, Dossi RC, Pare D, Oakson G. Fast oscillations (20–40 Hz) in thalamocortical systems and their potentiation by mesopontine cholinergic nuclei in the cat. Proc Natl Acad Sci U S A. 1991; 88:4396–4400. [PubMed: 2034679]

Steriade, M.; McCarley, RW. Brainstem control of wakefulness and sleep. Springer; New York, NY: 2005.

Steriade M, Nunez A, Amzica F. A novel slow (<1 Hz) oscillation of neocortical neurons *in vivo*: depolarizing and hyperpolarizing components. J Neurosci. 1993; 13:3252–3265. [PubMed: 8340806]

Takakusaki K, Habaguchi T, Ohtinata-Sugimoto J, Saitoh K, Sakamoto T. Basal ganglia efferents to the brainstem centers controlling postural muscle tone and locomotion: a new concept for understanding motor disorders in basal ganglia dysfunction. Neuroscience. 2003; 119:293–308. [PubMed: 12763089]

Takakusaki K, Shiroyama T, Kitai ST. Two types of cholinergic neurons in the rat tegmental pedunculopontine nucleus: electrophysiological and morphological characterization. Neuroscience. 1997; 79:1089–1109. [PubMed: 9219969]

Takakusaki K, Shiroyama T, Yamamoto T, Kitai ST. Cholinergic and noncholinergic tegmental pedunculopontine projection neurons in rats revealed by intracellular labeling. J Comp Neurol. 1996; 371:345–361. [PubMed: 8842892]

Volgushev M, Chauvette S, Mukovski M, Timofeev I. Precise long-range synchronization of activity and silence in neocortical neurons during slow-wave oscillations [corrected]. J Neurosci. 2006; 26:5665–5672. [PubMed: 16723523]

Wang HL, Morales M. Pedunculopontine and laterodorsal tegmental nuclei contain distinct populations of cholinergic, glutamatergic and GABAergic neurons in the rat. Eur J Neurosci. 2009; 29:340–358. [PubMed: 19200238]

Europe PMC Funders Author Manuscripts

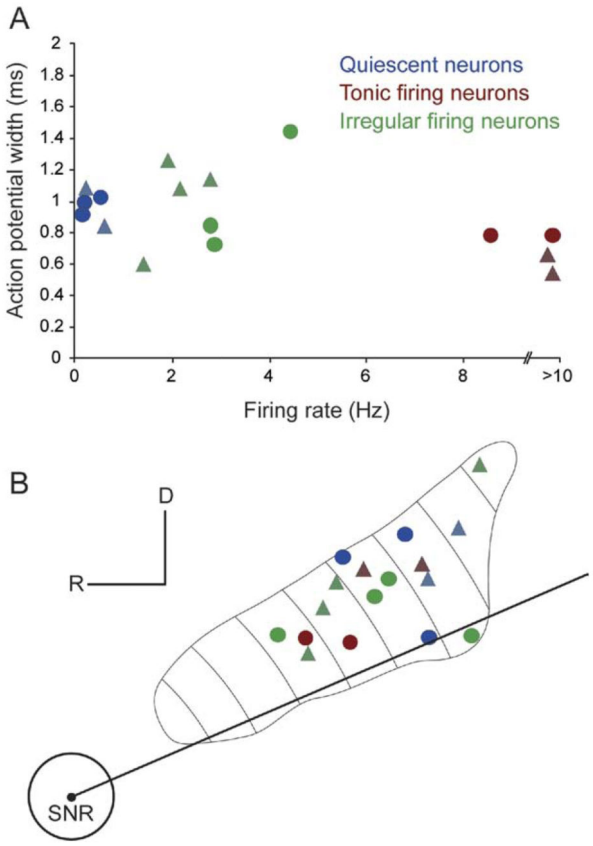

Fig. 1. Topographical distribution of physiologically identified neurobiotin-labeled neurons in the PPN.

(A) Some physiological parameters were useful to set the criteria for separation of neuronal subtypes in the PPN, such as firing rate during neocortical slow oscillations or coefficient of variation, while others were less effective, such as action potential width. (B) Labeled neurons were spread across the entire rostro-caudal and medio-lateral extent of the PPN, although quiescent neurons were only observed in the caudal half of the PPN. One non-cholinergic neuron was not electrophysiologically evaluated. Circles represent identified non-cholinergic neurons; triangles, non-identified neurons; blue, quiescent neurons; red, tonic firing neurons; green, irregular firing neurons.

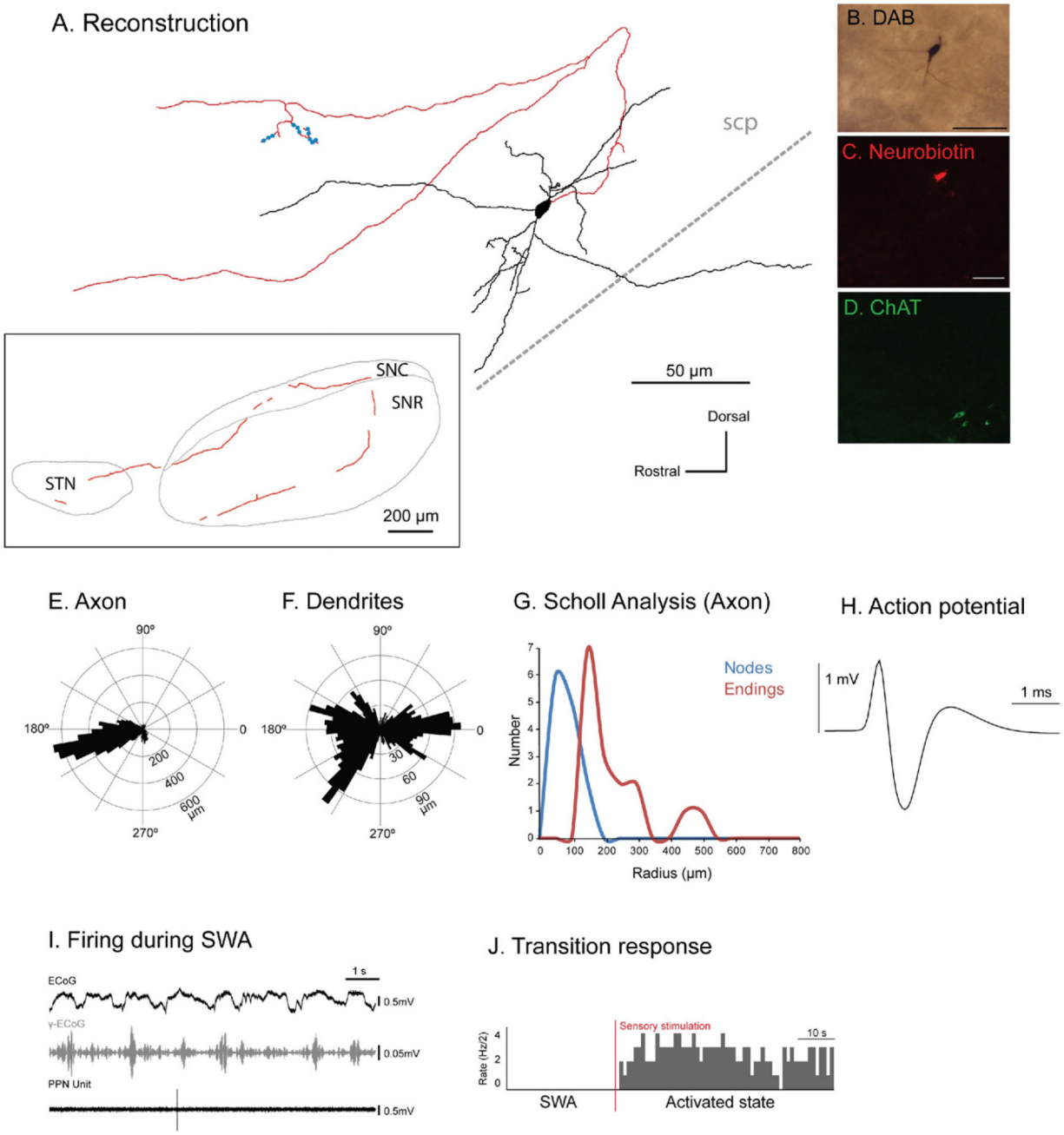

Fig. 2. Immunohistochemically identified quiescent non-cholinergic PPN neurons increase their activity during transitions from slow oscillations to global activation.

(A) Reconstruction of the cell body, dendrites (black) and axon (red) of an individual quiescent non-cholinergic PPN neuron (varicosities shown in blue). These neurons typically gave rise to an axon that emerged caudally from the cell body, formed a “loop” and traveled rostrally, giving rise to two ventral branches and collateralizing within the basal ganglia nuclei (see inset), namely the substantia nigra pars reticulata (SNR), substantia nigra pars compacta (SNC), and subthalamic nucleus (STN). The axon was traced as far as the STN, having traveled laterally and rostrally for a distance of ~3 mm. All quiescent neurons had

Europe PMC Funders Author Manuscripts

ascending axonal projections. (B–D) PPN neurons were juxtacellularly labeled (B) and identified as non-cholinergic by the lack of co-localization of fluorescent markers for neurobiotin (C) and ChAT immunoreactivity (D). (E, F) Polar histograms show direction of arborizations in the sagittal plane of the axon (E) and dendrites (F). (G) Axonal Scholl analysis shows the number of nodes and endings relative to the distance (in μm) from the soma. (H) Average action potential shape (0.96 ms width). (I) During robust SWA, neocortical activity (ECoG; black) was dominated by a slow oscillation (~1 Hz), the active components of which supported nested gamma oscillations (30–50 Hz; γ-ECoG, grey). This non-cholinergic neuron fired at a very low frequency (<1 Hz) and did not fire in time with the neocortical slow oscillation (top trace). (J) Example of induced activation of this quiescent neuron during the transition from neocortical slow oscillations to the activated state. Shortly after the onset of a hind paw pinch (indicated by the vertical bar; sensory stimulation, red), the majority of quiescent neurons increased their firing rate (n=3; data shown as spike count per 500 ms bins). Scale bars in (B) 50 μm, and (C, D) 20 μm.

Europe PMC Funders Author Manuscripts

Europe PMC Funders Author Manuscripts

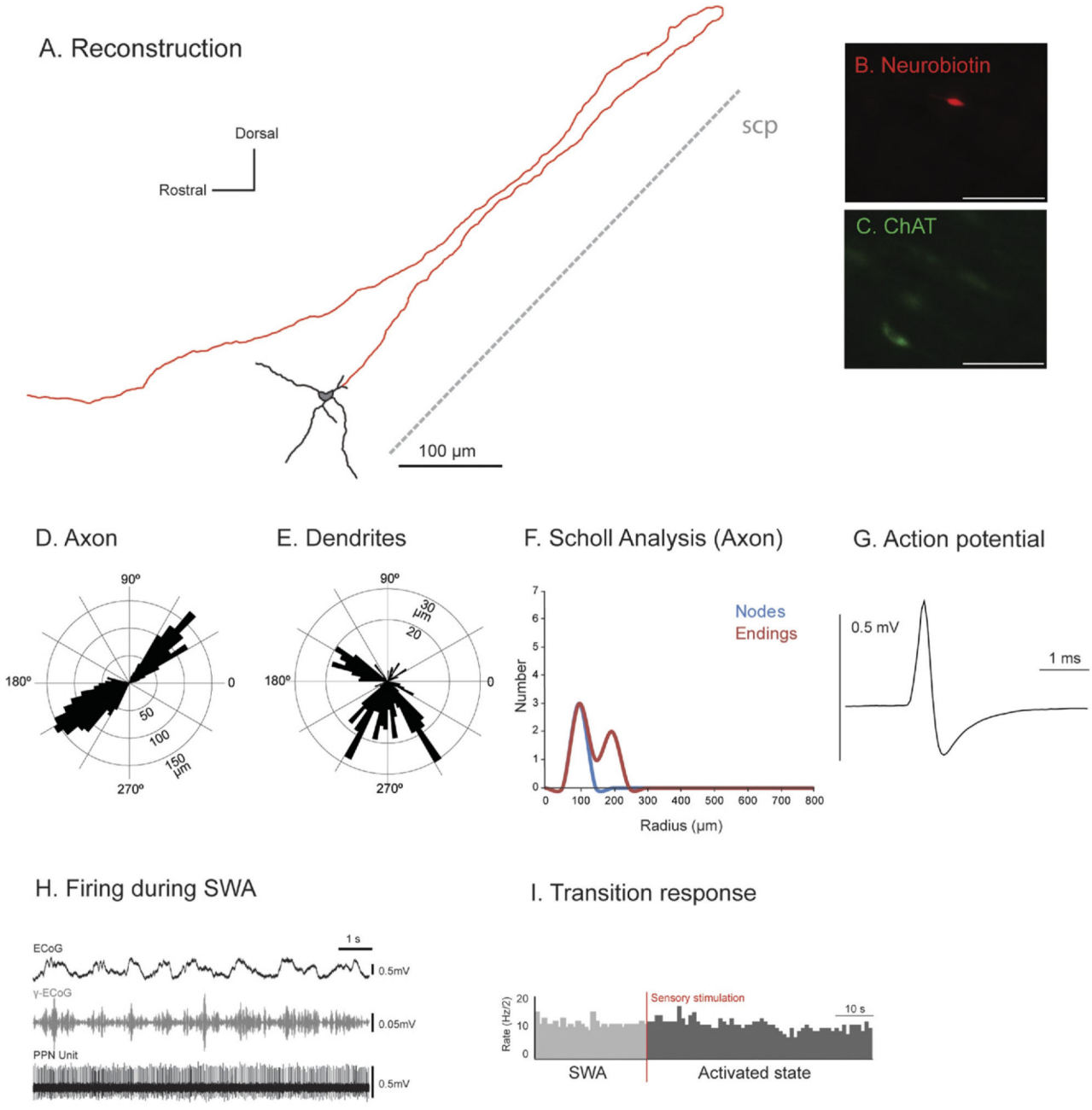

Fig. 3. Tonic non-cholinergic PPN neurons do not modify their activity during transitions from slow oscillations to global activation.

(A) Reconstruction of the cell body, dendrites (black) and axon (red) of an individual tonic non-cholinergic PPN neuron. These neurons typically gave rise to an axon that emerged caudally from a secondary dendrite, formed a “loop” and traveled rostrally giving rise to an ascending axonal projection. (B, C) PPN neurons were juxtacellularly labeled and identified as non-cholinergic by the lack of co-localization of fluorescent markers for neurobiotin (B) and ChAT immunoreactivity (C). (D, E) Polar histograms show direction of arborizations in the sagittal plane of the axon (D) and dendrites (E). (F) Scholl analysis shows the number of nodes and endings relative to the distance (in μm) from the soma. (G) Average action

potential shape (0.78 ms width). (H) During robust SWA, neocortical activity (ECoG; black) was dominated by a slow oscillation (~1 Hz), the active components of which supported nested gamma oscillations (30–50 Hz; γ-ECoG, grey). This non-cholinergic neuron fired at a high frequency (22 Hz) and did not show any preferential firing during the phases of the neocortical slow oscillation (top trace). (I) FR of the same tonic firing neuron during the transition from neocortical slow oscillations to an activated state (indicated by the vertical bar; sensory stimulation, red), showing that tonic neurons do not significantly change their FR (three of four). Scale bars: 100 μm.

Europe PMC Funders Author Manuscripts

Europe PMC Funders Author Manuscripts

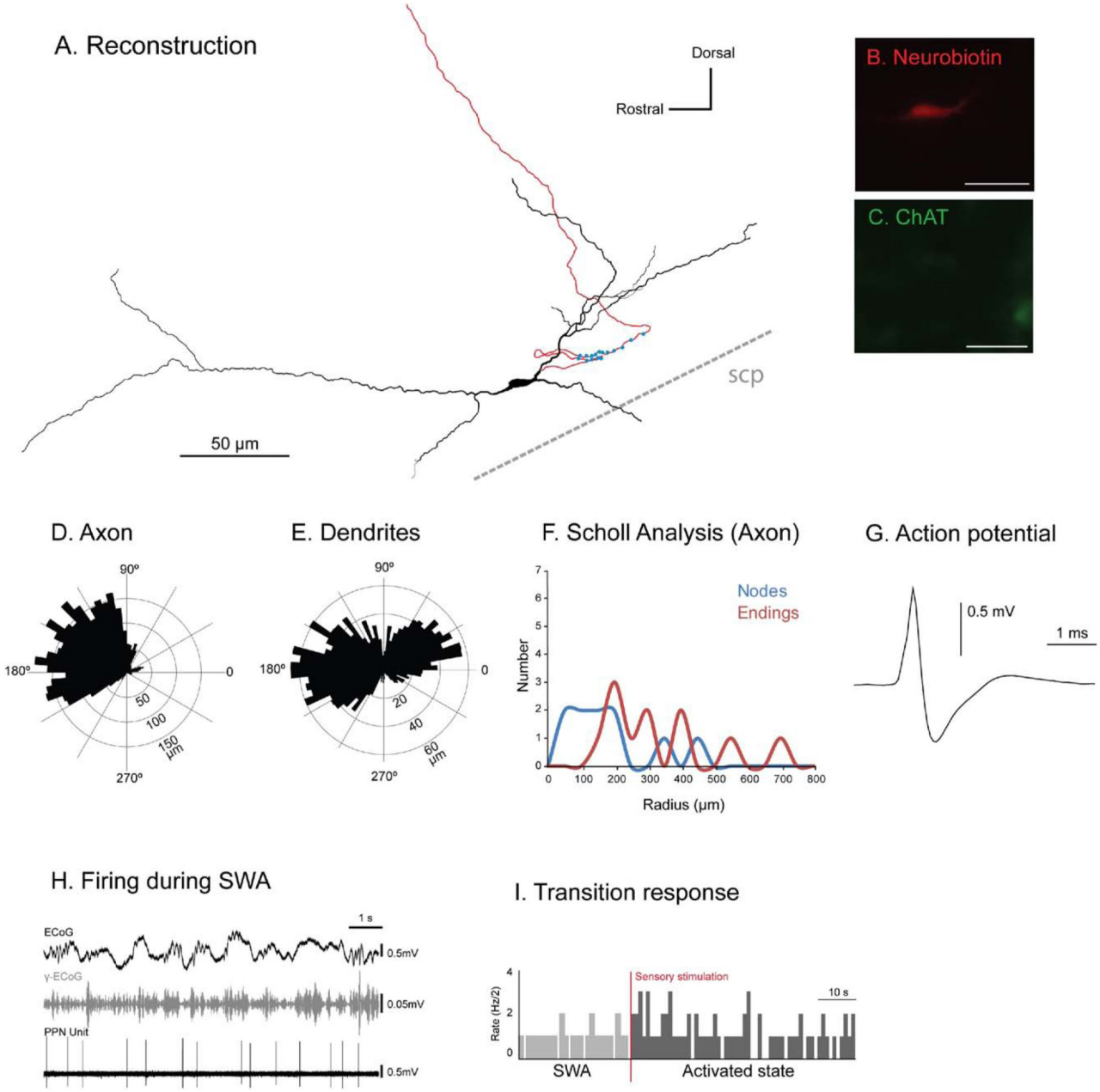

Fig. 4. Irregular non-cholinergic PPN neurons are heterogeneous in their activity during transitions from slow oscillations to global activation.

(A) Reconstruction of the cell body, dendrites (black) and axon (red) of an individual irregular firing non-cholinergic PPN neuron (varicosities shown in blue). These neurons typically gave rise to an axon that emerged caudally from a primary dendrite; this neuron gave rise to an axon that formed two “loops” and had a dorsally ascending axon. (B, C) PPN neurons were juxtacellularly labeled and identified as non-cholinergic by the lack of co-localization of fluorescent markers for neurobiotin (B) and ChAT immunoreactivity (C). (D, E) Polar histograms show direction of arborizations in the sagittal plane of the axon (D) and dendrites (E). (F) Scholl analysis shows the number of nodes and endings relative to the

distance (in μm) from the soma. (G) Average action potential shape (0.84 ms width). (H) During robust SWA, neocortical activity (ECoG; black) was dominated by a slow oscillation (~1 Hz), the active components of which supported nested gamma oscillations (30–50 Hz; γ-ECoG, grey). This non-cholinergic neuron fired at a frequency of 2.8 Hz during SWA. (I) Shortly after the onset of a hind paw pinch (indicated by the vertical bar; sensory stimulation, red), irregular neurons were highly heterogeneous in their responses, ranging from no response to moderate or strong responses and from excitation to inhibition. This neuron did not show a significant change in its FR following the pinch. Scale bars in (A) 50 μm, and (B, C) 20 μm.

Europe PMC Funders Author Manuscripts

Europe PMC Funders Author Manuscripts

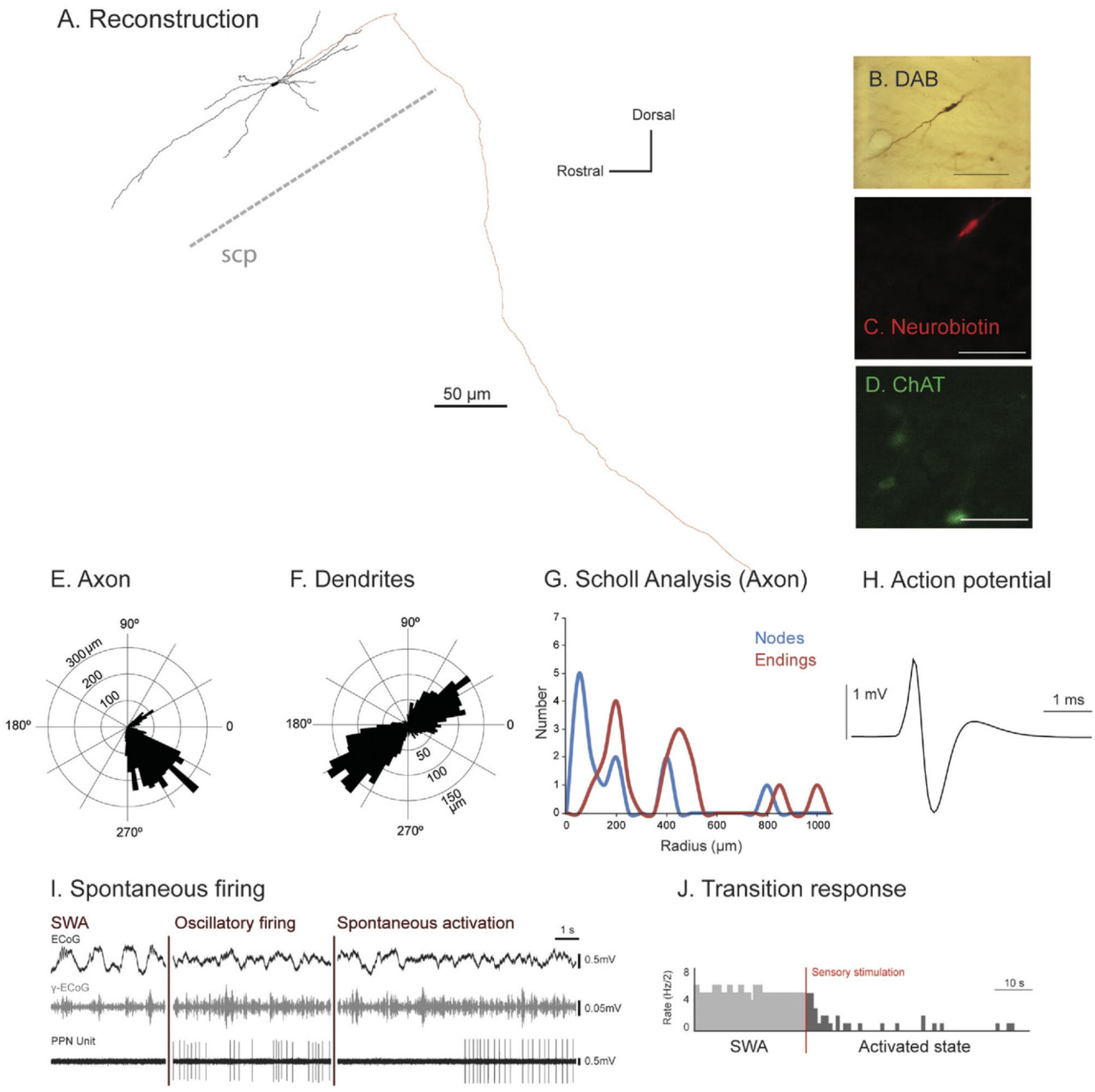

Fig. 5. Irregular firing descending-axon non-cholinergic PPN neurons show variable patterns of activity across different brain states.

(A) Reconstruction of the cell body, dendrites (black) and axon (red) of an individual irregular firing non-cholinergic PPN neuron. These neurons typically gave rise to an axon that emerged caudally from a primary dendrite; this neuron had a descending-only projection and did not give rise to any local boutons within the PPN. (B–D) PPN neurons were juxtacellularly-labeled (B) and identified as non-cholinergic by the lack of co-localization of fluorescent markers for neurobiotin (C) and ChAT immunoreactivity (D). (E, F) Polar histograms show direction of arborizations in the sagittal plane of the axon (E) and dendrites (F). (G) Scholl analysis shows the number of nodes and endings relative to the

distance (in μm) from the soma. (H) Average action potential shape (0.72 ms width). (I) During robust slow-wave activity, neocortical activity (ECoG; black) was dominated by a slow oscillation (~1 Hz), the active components of which supported nested gamma oscillations (30–50 Hz; γ-ECoG, grey). This non-cholinergic neuron showed spontaneous periods of silence alternated with stereotyped activity and showed no clear temporal relationship to the neocortical slow oscillation (top trace). (J) Example of induced cortical activation of the same PPN non-cholinergic neuron during the transition from neocortical slow oscillations to an activated state. Shortly after the onset of a hindpaw pinch this neuron was inhibited. Scale bars in (B) 50 μm, and (C, D) 20 μm.

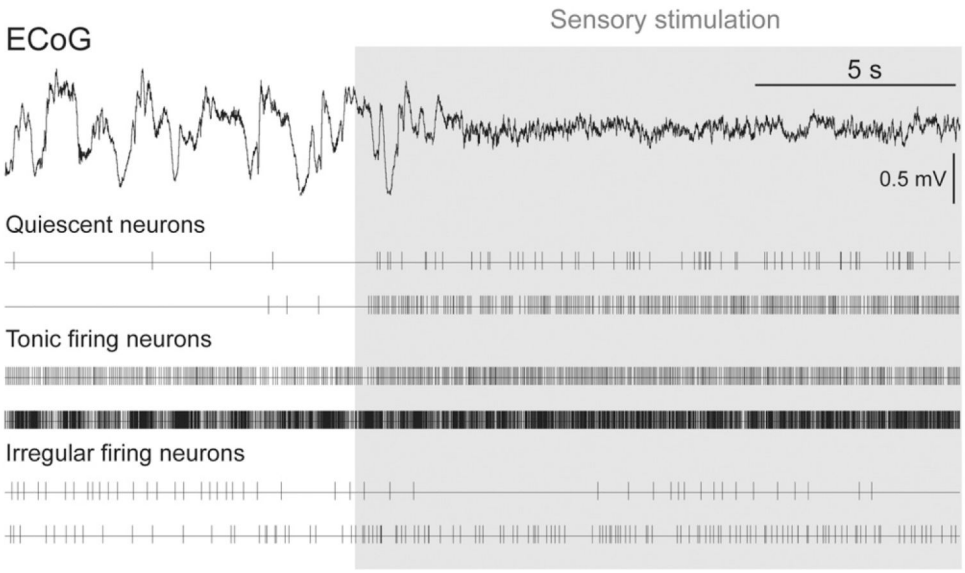

Fig. 6. Different patterns of activity in PPN neurons occur in parallel during slow-wave activity.

Neurons in the PPN were recorded simultaneously using high-density multielectrodes across different dorso-ventral locations. Two examples of each neuronal subgroup (quiescent, tonic firing and irregular firing neurons) are depicted as events in order to show the range of properties and responses within the distinct groups.

Europe PMC Funders Author Manuscripts

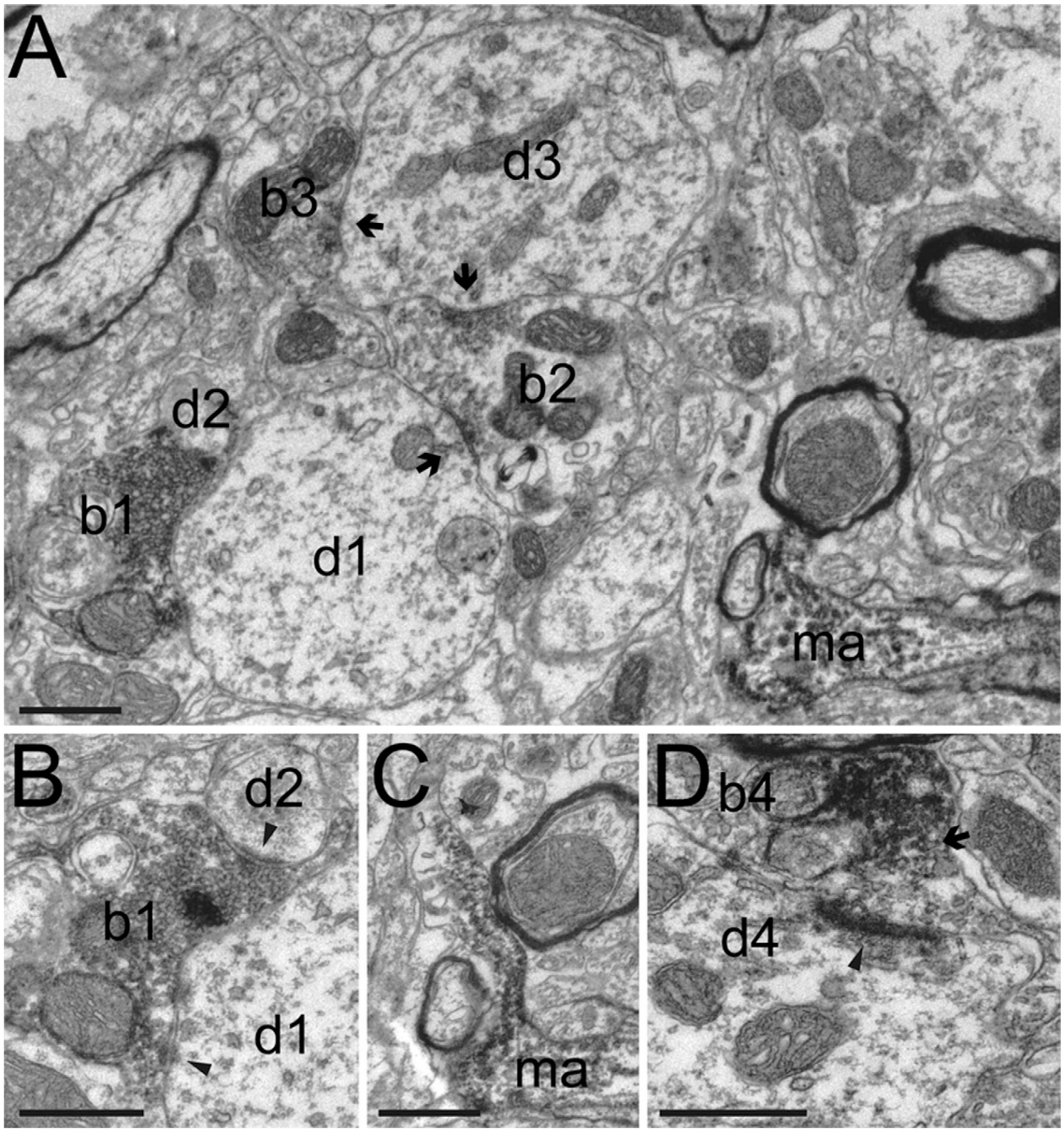

Fig. 7. Local synaptic contacts formed by non-cholinergic neurons of the PPN.

(A–B) A labeled bouton of a local PPN neuron (b1) forms asymmetrical synaptic contacts (panel B, arrowheads) with two dendrites (d1 and d2). An unlabeled bouton (b2), forms symmetrical synaptic contacts (arrows) with two dendrites of a similar size (d1 and d3), the second of which is in an asymmetrical synaptic contact (arrow) with a third (unlabeled) bouton (b3). (C) Another part of the same labeled axon that forms bouton b1 is seen to be myelinated in Panel (A) (ma), which was typical of the axon when it was not forming synaptic contacts. In this serial section an axonal process sprouts from a gap in the myelin.

(D) A labeled bouton (b4), originating from the same axon, but approximately 75 μm away, makes asymmetrical synaptic contact (arrowhead) with a dendrite (d4). Note how the labeling is only present at the neck of the bouton (arrow), away from the synapse. This could indicate the limit of neurobiotin diffusion within the axon. Scale bars: 0.5 μm.

Europe PMC Funders Author Manuscripts

Europe PMC Funders Author Manuscripts

Table 1

Summary of the morphological and physiological properties of the three categories of PPN neurons

Neuronal type	Cell body area (μm^2)	Total number dendritic beads	Number of local boutons	Axon origin	Total dendritic length (μm)	firing rate SWA (Hz)	firing rate AS (Hz)	CV SWA	CV AS	AP width (ms)	firing rate response to brain state transitions		
											Increase	Decrease	No change
Quiescent neurons (*n*=5)	277±28	18.8±9.3	36&11 (*n*=2)	Cell body (*n*=3)	2514±478	0.27±0.1	1.75±0.9	1.13±0.13	0.59±0.16	0.95±0.02	3	1	1
Tonic firing neurons (*n*=4)	185±43	0 (*n*=3) & 46 (*n* = 1)	0	Secondary dendrite (*n*=3)	2002±599	19.14±3.54	22.02±3.21	0.27±0.01	0.32±0.03	0.69±0.06	1	0	3
Irregular firing neurons (*n*=8)	225±27	40.6±22.9 (*n*=7)	16&24 (*n*=2)	Primary dendrite (*n*=4)	3534±443	2.62±0.27 (*n*=7)	3.04±0.86 (*n*=7)	0.71±0.15 (*n*=7)	0.91±0.22 (*n*=7)	1.01±0.08 (*n*=7)	4*	1	2

Displayed values are averages ± SEM for all neurons in each group unless otherwise stated.

AP, action potential; AS, activated state; CV, coefficient of variation; SWA, slow-wave activity.

*Two of these neurons showed a bimodal response, that is, they decreased their firing rate following their initial increase.